Electronic Supplementary Material (ESI) for Dalton Transactions.


# Supporting Information

## σ-Hole triel bonds in aluminium derivatives

Vanessa Tabernero,[a] Teresa Muñoz,[a] Miguel Palenzuela,[a] Rosa M. Gomila,[b] Antonio Frontera,*[b] and Marta E. G. Mosquera,*

[a]Department of Organic and Inorganic Chemistry, Institute of Chemical Research "Andrés M. del Río" (IQAR), Universidad de Alcalá, Campus Universitario, 28871 Alcalá de Henares, Madrid (Spain). e-mail: martaeg.mosquera@uah.es

bDepartment of Chemistry, Universitat de les Illes Balears, Crta. Valldemossa km 7.5, 07122 Palma de Mallorca, Spain. e-mail: toni.frontera@uib.es

## 1. Experimental section

### General considerations

All manipulations were carried out under an inert atmosphere of argon by using standard Schlenk and glovebox techniques. All solvents were rigorously dried prior to use by following standard methods. NMR spectra were recorded at 400.13 ($^1$H) and 100.62 ($^{13}$C) MHz with a Bruker AV400 and a Varian NMR System 500 multinuclear. Chemical shifts ($\delta$) are given in ppm using $C_6D_6$ as solvent. $^1$H and $^{13}$C resonances were measured relative to solvent peaks considering TMS $\delta$ = 0 ppm. All reagents were commercially obtained and used without further purification. Compound **2** was prepared as reported by us.[1]

### Synthesis of [AlMe$_2${2,6-(MeO)$_2$C$_6$H$_3$O}(DMSO)] (1).

To a solution of compound [AlMe$_2${2,6-(MeO)$_2$C$_6$H$_3$O}]$_2$ (**2**) (0.50 g, 1.19 mmol) in 20 mL of toluene 0.17 mL (2.38 mmol) of DMSO were added at room temperature. The solution was stirrer for 2 days and then the solvent removed to half its volume under vacuum. After one day at −20 °C the formation of crystals corresponding to compound **1** is observed. Yield: 67.8 % (0.46 g, 1.61 mmol). $^1$H-NMR (500 MHz, 293 K, tol-d$_8$): δ −0.41 (s, 6H, AlC*H*$_3$), 2.05 (s, SC*H*$_3$), 3.50 (s, 6H, OC*H*$_3$), 6.42 (d, 2H, $^3J_{HH}$ = 8 Hz, *m*-OAr-*H*), 6.58 (t, 1H, $^3J_{HH}$ = 8 Hz, *p*-OAr-*H*). $^1$H-NMR (400 MHz, 293 K, $C_6D_6$): δ −0.23 (s, 6H, AlC*H*$_3$), 1.95 (s, 6H, SC*H*$_3$), 3.51 (s, 6H, OC*H*$_3$), 6.50 (d, 2H, $^3J_{HH}$ = 8 Hz, *m*-OAr-*H*), 6.67 (t, 1H, $^3J_{HH}$ = 8 Hz, *p*-OAr-*H*). $^{13}$C{$^1$H} NMR (100,6 MHz, 293 K, $C_6D_6$): δ −8.23 (s, Al*C*H$_3$), 37.70 (s, S*C*H$_3$), 55.17 (s, O*C*H$_3$), 105.75 (s, *m*-Ph), 115.16 (s, *p*-Ph), 141.47 (s, *i*-OAr), 150.21 (s, *o*-OAr). Anal. Calc. (%) for AlC$_{12}$H$_{21}$O$_4$S (288,33 g/mol): C, 49.94; H, 7.28. Exp.: C, 50.09; H, 7.07.

### Single-Crystal X-ray Structure Determination for 1.

Data collection was performed at 200(2) K, with the crystals covered with perfluorinated ether oil. Single crystals of **1** were mounted on a Bruker-Nonius Kappa CCD single crystal diffractometer equipped with a graphite-monochromated Mo-Kα radiation (λ = 0.71073 Å). Multiscan[2] absorption correction procedures were applied to the data. The structure was solved using the WINGX package,[3] by direct methods (SHELXS-97) and refined using full-matrix least-squares against $F^2$ (SHELXL-97).[4] All non-hydrogen atoms were anisotropically refined. Hydrogen atoms were geometrically placed and left riding on their parent atoms. Full-matrix least-squares refinements were carried out by minimizing $\sum w(Fo^2 - Fc^2)^2$ with the SHELXL-97 weighting scheme and stopped at shift/err < 0.001. The final residual electron density maps showed no remarkable features. Crystallographic data for the structure reported in this paper have been deposited with the Cambridge Crystallographic Data Centre as supplementary publication no. CCDC- 2217231 [1].

## 2. Spectroscopic data for 1

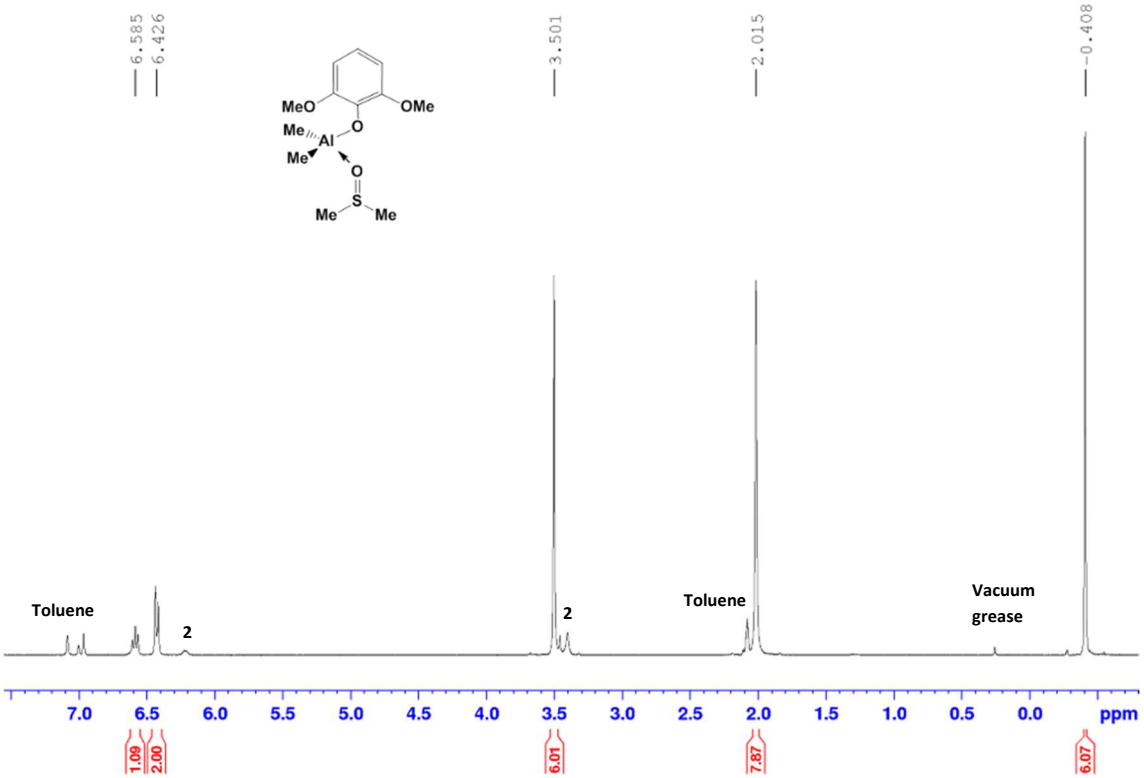


**Figure S1** $^{1}$H (500 MHz, toluene-$d_8$) NMR spectrum of compound **1.**

The impurities observed come from the parent dinuclear species [$AlMe_2${2,6-$(MeO)_2C_6H_3O$}]$_2$ (**2**), even if the NMR is done from crystals or in the presence of an excess of DMSO, a small amount from the parent compound is observed, which may imply the existence of an equilibrium of coordination/discoordination of the DMSO.

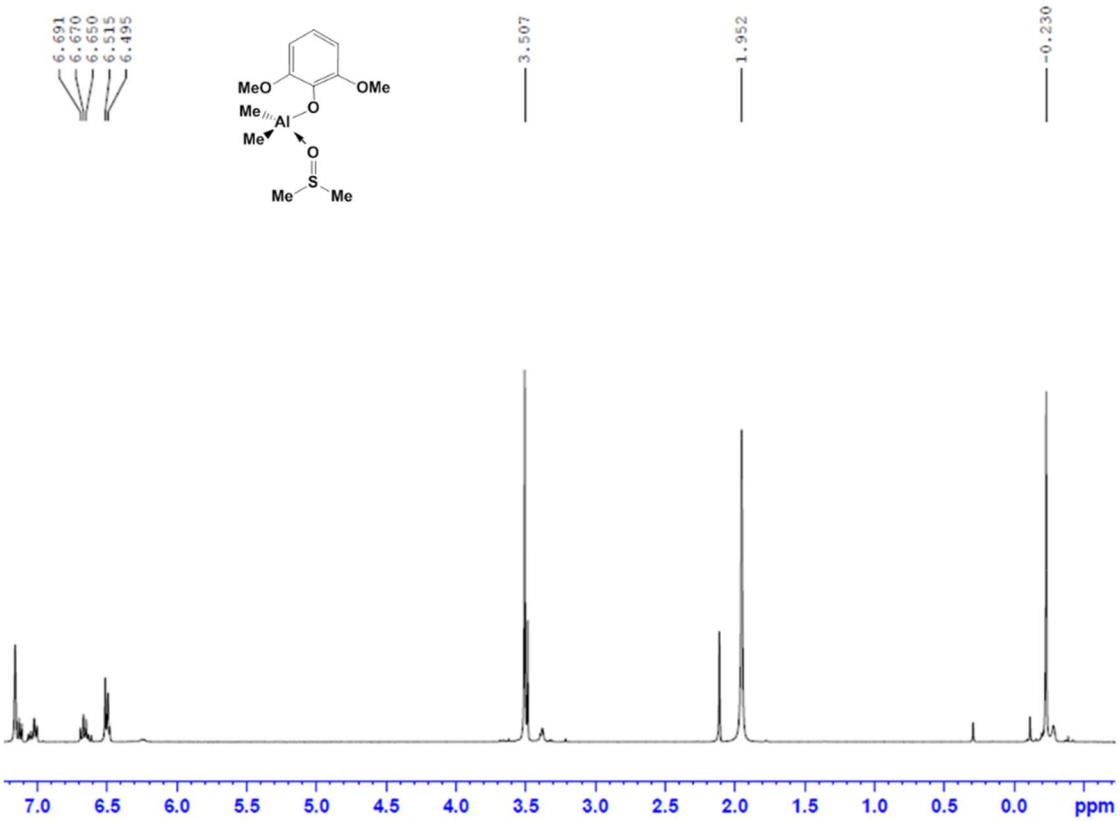


**Figure S2** $^{1}H$ (400 MHz, $C_6D_6$) NMR spectrum of compound **1**

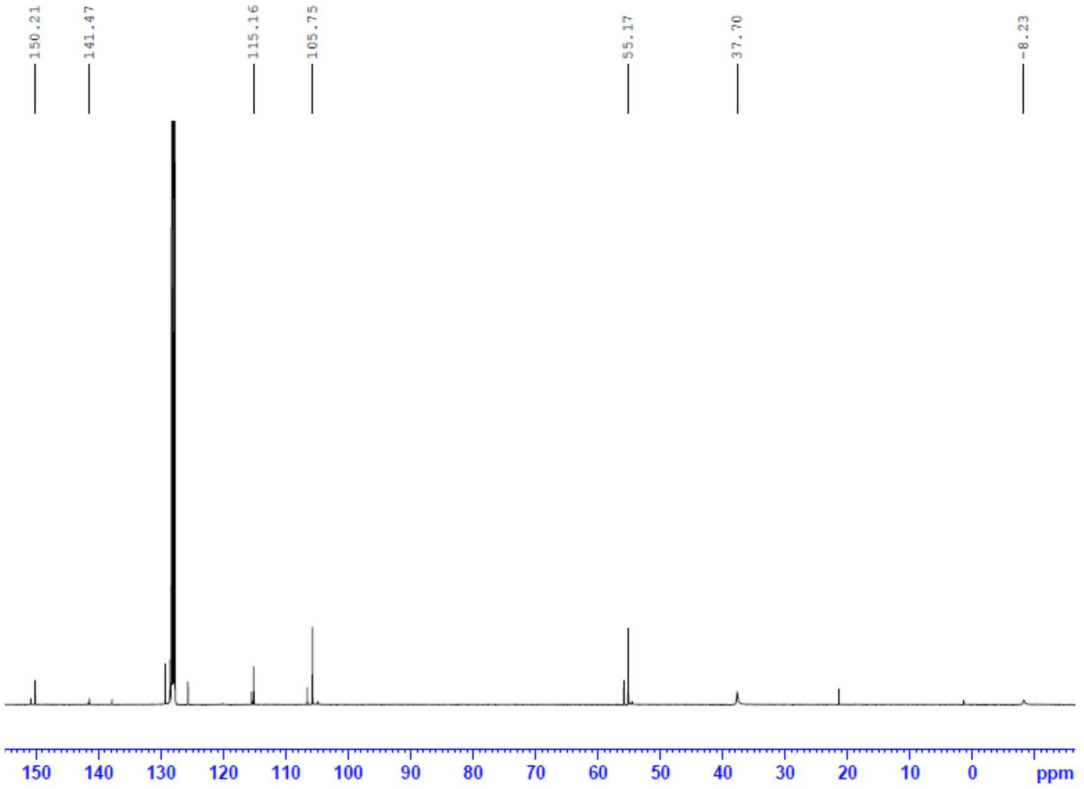


**Figure S3.** $^{13}C\{^{1}H\}$ (100.6 MHz, $C_6D_6$) NMR spectrum of compound **1**

## 3. Low temperature NMR experiments

Low temperature NMR experiments had been performed in toluene-$d_8$ down to -70°C but the non-equivalence of the OMe had not been observed, so this TrB cannot be evaluated spectroscopically in solution.

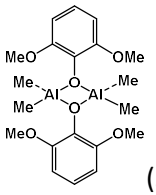


(**2**)

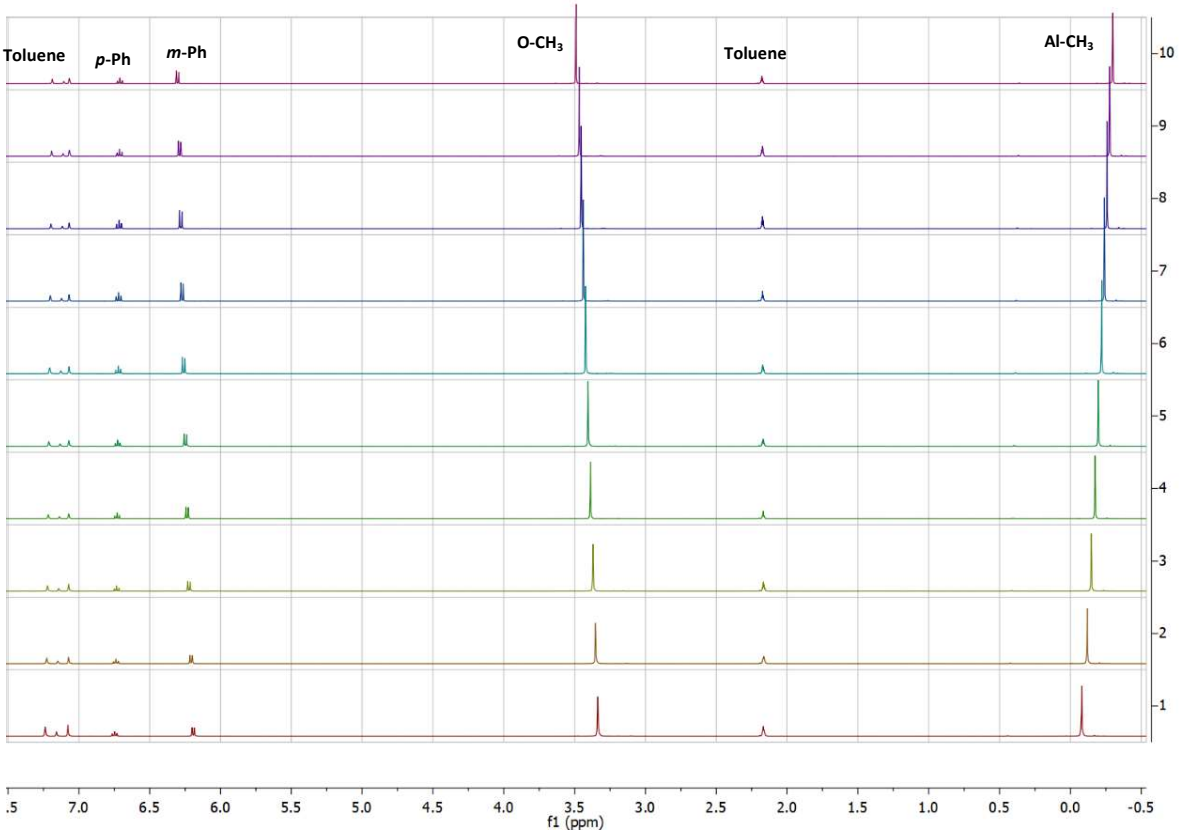


**Figure S4.** Low temperature $^1$H (500 MHz, toluene-$d_8$) NMR spectra for **2**. A spectrum had been recorded every 10°C, from room temperature to -70 °C (Top to bottom). The peaks over 7 ppm and at 2.21 ppm corresponds to the signals for the residual non-deuterated toluene.

For compound **2** there is a shift of the signals that can be attributed to the anisotropic effects and interactions with the aromatic rings of the solvent. The methyl groups bonded to the aluminum are deshielded while the OMe moved in the opposite way. This behavior can be attributed to anisotropic effects caused by the different orientations of the surrounding solvent molecules. Depending on the orientation of the aromatic ring of the toluene molecules the peaks can be shielded or deshielded and since the Me groups and the OMe groups are in near perpendicular planes (angle 85.5°) it could be expected that both groups behave in a different way. This behavior may imply that when lowering the temperature, the solvent arranges differently in relation to compound **2**. As well the peaks for the aromatic protons corresponding to the residual non-deuterated toluene modify when lowering the temperature.

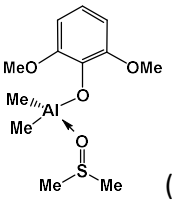


(**1**)

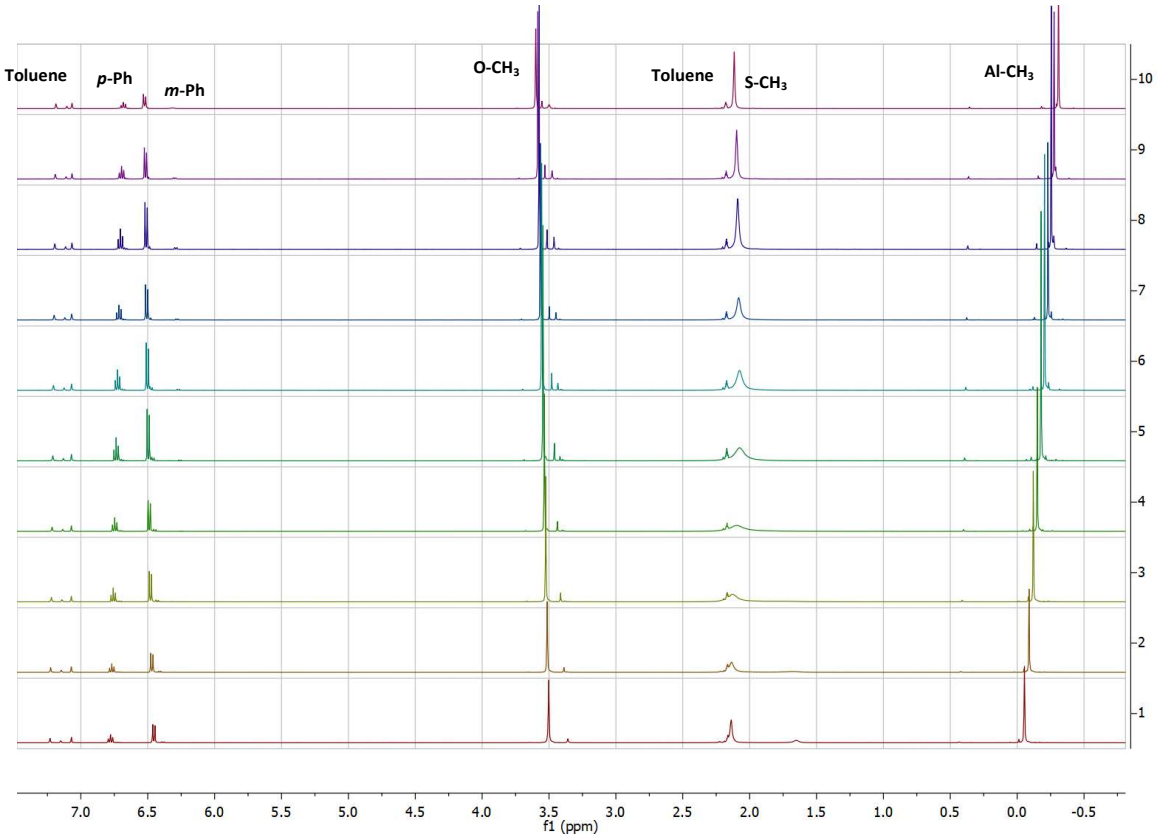


**Figure S5.** Low temperature $^{1}H$ (500 MHz, toluene-$d_8$) NMR spectra for **1**. A spectrum had been recorded every 10°C, from room temperature to -70 °C (Top to bottom). The peaks over 7 ppm and at 2.21 ppm corresponds to the signals for the residual non-deuterated toluene.

As similar behavior was observed for **1**, but in this case the DMSO peak modifies as the temperature goes down which could be in agreement with a process of coordination and discoordination in solution. In fact, at -60°C a new peak at 1.6 ppm is observed that can be assigned to uncoordinated DMSO. Remarkable the signals shift significantly when changing the solvent from benzene to toluene, which reflects the significant effect of the aromatic solvent on the NMR spectroscopic behavior of these species.

## 4. Single-Crystal X-ray Data for 1.

**Table S1** Crystallographic data for **[$AlMe_2${2,6-$(MeO)_2C_6H_3O$}(DMSO)]** (**1**)

| | **[$AlMe_2${2,6-$(MeO)_2C_6H_3O$}(DMSO)]** |
|---|---|
| Empirical formula | $AlC_{12}H_{21}O_4S$ |
| Formula weight | 288.33 |
| Colour, shape | Colourless/block |
| Crystal size (mm) | 0.49 x 0.41 x 0.39 |
| Crystal system | Orthorhombic |
| Space group | *Pbca* |
| *a* (Å) | 14.2726(17) |
| *b* (Å) | 12.0903(17) |
| *c* (Å) | 17.953(2) |
| *V* (Å$^3$) | 3098.0(7) |
| *Z* | 8 |
| $\rho_{calcd.}$ (mg m$^{-3}$) | 1.236 |
| $F_{000}$ | 1232 |
| $\mu$ (mm$^{-1}$) | 0.269 |
| $\theta$ Range (°) | 3.17-27.50 |
| Reflns. Collected | 12768 |
| Indep. Reflns./R(int) | 3533/0.0664 |
| Data/restraints/param | 3533/0/163 |
| $R_1/wR_2$ ($I > 2\sigma(I)$) [a] | 0.0488/0.1319 |
| $R_1/wR_2$ (all data)[a] | 0.0987/ 0.1529 |
| GOF | 1.024 |
| Max/min $\Delta\rho$ (e.Å$^{-3}$) | 0.415/−0.434 |

[a] $R_1 = \Sigma(||F_o| - |F_c||)/\Sigma|F_o|$; $wR_2 = \{\Sigma[w(F_o^2 - F_c^2)^2]/\Sigma[w(F_o^2)^2]\}^{1/2}$; GOF = $\{\Sigma[w(F_o^2 - F_c^2)^2]/(n - p)\}^{1/2}$

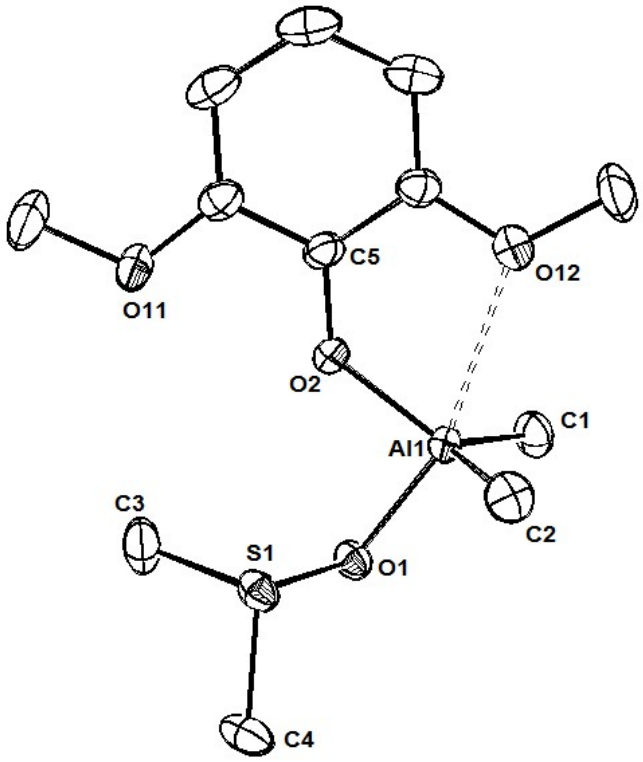


**Figure S3.** Ortep Diagram for compound [$AlMe_2${2,6-$(MeO)_2C_6H_3O$}(DMSO)] (**1**). Ellipsoid probability 30%, hydrogen atoms have been omitted for clarity.

**Table S2** Bond lengths (Å) and angles (°) for **[$AlMe_2${2,6-$(MeO)_2C_6H_3O$}(DMSO)]** (**1**)

| **Bond lengths (Å)** | | | |
|---|---|---|---|
| S(1)-O(1) | 1.5352(17) | O(11)-C(11) | 1.420(4) |
| S(1)-C(3) | 1.769(4) | C(5)-C(6) | 1.397(4) |
| S(1)-C(4) | 1.769(3) | C(5)-C(10) | 1.390(4) |
| Al(1)-O(2) | 1.773(2) | C(6)-C(7) | 1.391(4) |
| Al(1)-O(1) | 1.8973(18) | C(10)-C(9) | 1.383(4) |
| Al(1)-C(1) | 1.955(3) | C(10)-O(12) | 1.372(3) |
| Al(1)-C(2) | 1.961(3) | O(12)-C(12) | 1.415(3) |
| O(2)-C(5) | 1.340(3) | C(9)-C(8) | 1.378(5) |
| O(11)-C(6) | 1.363(4) | C(7)-C(8) | 1.376(5) |
| **Bond lengths (Å)** | | | |
| O(1)-S(1)-C(3) | 104.77(15) | O(2)-C(5)-C(6) | 120.0(3) |
| O(1)-S(1)-C(4) | 102.70(12) | O(2)-C(5)-C(10) | 121.1(2) |
| C(3)-S(1)-C(4) | 100.33(18) | C(6)-C(5)-C(10) | 118.9(3) |
| O(2)-Al(1)-O(1) | 90.45(9) | O(11)-C(6)-C(5) | 115.1(2) |

| | | | |
|---|---|---|---|
| O(2)-Al(1)-C(1) | 118.35(13) | O(11)-C(6)-C(7) | 125.6(3) |
| O(1)-Al(1)-C(1) | 101.41(11) | C(5)-C(6)-C(7) | 119.3(3) |
| O(2)-Al(1)-C(2) | 115.20(13) | C(9)-C(10)-O(12) | 125.5(3) |
| O(1)-Al(1)-C(2) | 102.21(11) | C(9)-C(10)-C(5) | 122.0(3) |
| C(1)-Al(1)-C(2) | 120.50(14) | O(12)-C(10)-C(5) | 112.5(2) |
| S(1)-O(1)-Al(1) | 116.48(10) | C(10)-O(12)-C(12) | 118.7(3) |
| C(5)-O(2)-Al(1) | 130.47(18) | C(10)-C(9)-C(8) | 118.0(3) |
| C(6)-O(11)-C(11) | 117.8(3) | C(6)-C(7)-C(8) | 120.1(3) |
| | | C(9)-C(8)-C(7) | 121.7(3) |

## 4. Theoretical calculations.

The energies and wavefunction calculations of the supramolecular assemblies investigated in this manuscript were performed at the RI-PBE0[5]-D3[6]/def2-TZVP[7] level of theory using the Turbomole 7.2 program[8] either the crystallographic coordinates or fully optimized geometries. The noncovalent interaction (NCI) plot[9] were used to characterize the NCIs by representing the reduced density gradient (RGD) isosurfaces, which are very convenient to reveal noncovalent interactions in real space. The cubes needed to construct the NCIplot surfaces were generated from the wavefunctions by means of the MULTIWFN program.[10] The RDG isosurfaces correspond to both favorable and unfavorable interactions, as differentiated by the sign of the second density Hessian eigenvalue and defined by the isosurface color and were represented using VMD software.[11]

## 5. References.


1. M. T. Muñoz, T. Cuenca and M. E. G. Mosquera, *Dalton Trans*., 2014, **43**, 14377

2.R. H. Blessing, *SORTAV, Acta Cryst.,* 1995, **A51,** 33.

3.L. J. Farrugia, *J. Appl. Cryst.,* 1999, **32**, 837.

4.G. M. Sheldrick, *Acta Crystallogr. Sect. A* 2008*,* **A64**, 112; G. M. Sheldrick, *Acta Crystallogr.,* 2015, **C71**, 3-8.

5. C. Adamo and V. Barone, *J. Chem. Phys*., 1999, **110**, 6158-6169.

6. S. Grimme, J. Antony, S. Ehrlich, H. Krieg, *J. Chem. Phys*., 2010, **132**, 154104.

7. F. Weigend, *Phys. Chem. Chem. Phys*., 2006, **8**, 1057.

8. R. Ahlrichs, M. Bär, M. Hacer, H. Horn and C. Kömel, *Chem. Phys. Lett*., 1989, **162**, 165.

9. J. Contreras-Garcia, E. R. Johnson, S. Keinan, R. Chaudret, J. P. Piquemal, D. N. Beratan and W. Yang, *J. Chem. Theory Comput*. 2011, 7, 625.

10. T. Lu and F. Chen, *J. Comput. Chem*., 2012, **33**, 580–592.

11. J. W. Humphrey, A. Dalke and K. Schulten, *J. Mol. Graph*., 1996, **14**, 33–38.